Chaos, Solitons and Fractals 148 (2021) 110992

Contents lists available at ScienceDirect

Chaos, Solitons and Fractals

Nonlinear Science, and Nonequilibrium and Complex Phenomena

journal homepage: www.elsevier.com/locate/chaos

Frontiers

A family of circulant megastable chaotic oscillators, its application for the detection of a feeble signal and PID controller for time-delay systems by using chaotic SCA algorithm

Karthikeyan Rajagopal[a], Murat Erhan Cimen[b], Sajad Jafari[c], Jay Prakash Singh[d], Binoy Krishna Roy[e], Omer Faruk Akmese[f], Akif Akgul[f,*]

[a] Center for Nonlinear Systems, Chennai Institute of Technology, India
[b] Department of Electrical and Electronics Engineering, Faculty of Technology, Sakarya University of Applied Sciences, Serdivan, Sakarya, Turkey
[c] Nonlinear Systems and Applications, Faculty of Electrical and Electronics Engineering, Ton Duc Thang University, Ho Chi Minh City, Vietnam
[d] Department of Electrical Engineering, VNIT, Nagpur, Maharashtra, 440010, India
[e] Department of Electrical Engineering, National Institute of Technology Silchar, Silchar, 788010, Assam, India
[f] Department of Computer Engineering, Faculty of Engineering, Hitit University, Corum, Turkey

A R T I C L E I N F O

Article history:
Received 16 January 2021
Revised 29 March 2021
Accepted 20 April 2021
Available online 24 May 2021

Keywords:
Nonlinear dynamics
Megastability oscillators
Circulant
Bifurcation
Feeble-signal detection
Metaheuristic algorithm
Pid
Time-delay system
Sine-cosine algorithm

A B S T R A C T

Chaotic systems with cyclic symmetry are very rare and have been less discussed in the literature. Similarly, megastable oscillators, which can have a finite or infinite number of coexisting attractors, have also attracted researchers. We propose a class of cyclic symmetry oscillators with the megastable property with infinite coexisting attractors for the first time in the literature. Various dynamical properties of the proposed oscillators are discussed in detail. An application for the detection of a feeble signal by using the proposed circulant megastable oscillator is presented. Since chaotic oscillators are highly sensitive to a tiny change in the parameters or an external input to the oscillator, this property of the proposed oscillator is used for the detection of a feeble signal. Simulated results validate the effectiveness of the proposed application. After that, a new chaotic Sine-Cosine Algorithm (SCA) is developed using the randomness of megastable oscillators. Subsequently, this new chaotic sine-cosine algorithm is used to determine the PID controller parameters of time-delay systems concerning the objective function. As a result, the proposed chaotic sine-cosine algorithm presents better performance for time-delay systems when compared with the available algorithms in the literature.

1. Introduction

A deterministic dynamical system with extremely irregular behavior is identified as chaos. Interestingly, few literatures documented symmetry in chaotic attractors; it helps us to understand the order and patterns in nature. Albeit snowflakes appear to contain randomness redolent of chaos, it keeps symmetry. Two fashions of symmetry are studied frequently. These are Cyclic symmetry and Reflective symmetry. A cyclic type of symmetry is formulated by n-fold rotations about a point. In contrast, a reflective or dihedral type is formulated by rotations and reflections through a line passing through the point of rotation. Field and Goubitsky [1] constructed chaotic attractors with symmetry property by reducing the equivariant complex function. They laid a platform to formulate chaotic systems with cyclic symmetric attractors. Recently, enormous works have been reported on cyclic symmetry; mostly, these systems used general polynomials or trigonometric functions. Brisson et al. [2] presented chaotic attractors with a cube shape symmetry structure. Reiter reported chaotic attractors with hypercube symmetry [3] and tetrahedral shape symmetry [4]. Dumont [5] discussed the frieze type and wallpaper symmetries. All these methods are limited to polynomial-based functions. Wang et al. [6] conducted experiments to formulate various symmetry using trigonometric functions. Additionally, they reported dihedral symmetries. Similar methods are identified to yield a significant number of esthetic patterns.

A particle moving in a three-dimensional lattice with frictional damping is modeled with state-space equations by interchanging the three orthogonal axes and investigating the property of cyclic symmetry. The route to chaos, multistability, chaotic diffusion, and

* Corresponding author.
E-mail addresses: akifakgul@hitit.edu.tr, akgulakif@gmail.com (A. Akgul).

https://doi.org/10.1016/j.chaos.2021.110992
0960-0779/

Table 1
A class of circulant-megastable oscillators.

System name	Model	Parameters	Figures
CMO-1	$\dot{x} = b\cos(y) - f(\omega)$ $\dot{y} = b\cos(z) - f(\omega)$ $\dot{z} = b\cos(w) - f(\omega)$ $\dot{w} = b\cos(x) - f(\omega)$	$a = 3, b = 1, \omega = 1$	Fig. 1a
CMO-2	$\dot{x} = \cos(y) - a\tanh(x)$ $\dot{y} = \cos(z) - a\tanh(y)$ $\dot{z} = \cos(w) - a\tanh(z)$ $\dot{w} = \cos(x) - a\tanh(w)$	$a = 0.2$	Fig. 1b
CMO-3	$\dot{x} = \cos(y) - b\tanh(x) - f(\omega)$ $\dot{y} = \cos(z) - b\tanh(y) - f(\omega)$ $\dot{z} = \cos(w) - b\tanh(z) - f(\omega)$ $\dot{w} = \cos(x) - b\tanh(w) - f(\omega)$	$a = 3, b = 0.2, \omega = 1$	Fig. 1c

where $f(\omega) = a\sin(\omega t)$is the forcing function. A periodic forcing, as described in the literature [10,14–16], is used in this paper. It is the simplest forcing function discussed in the literature and also easy to generate during hardware implementation. It can be easily verified that all the above three systems have an infinite number of equilibrium points.

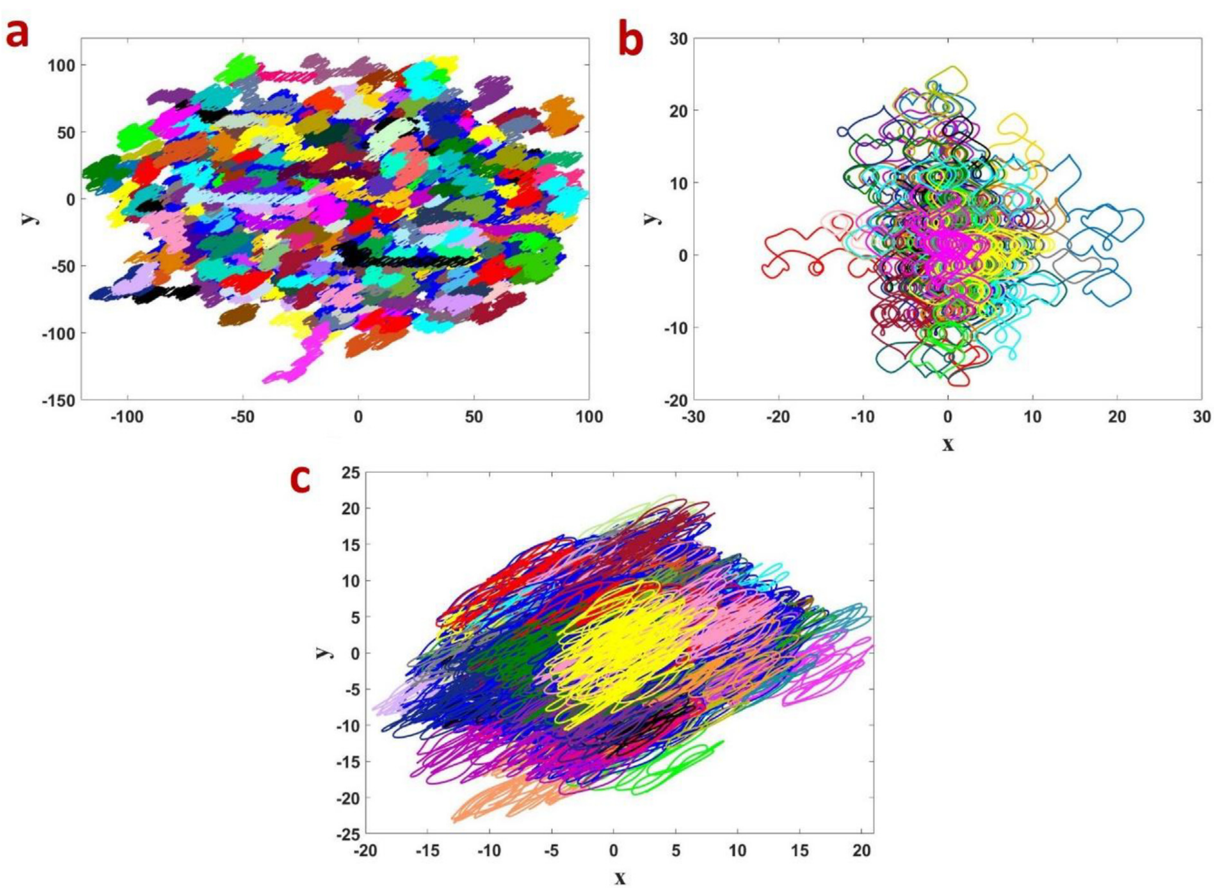

Fig. 1. Phase portrait of the CMO systems for various initial conditions located on the x-axis (a: from $x = -100$ to $x = +100$ with steps equal to 2; b: from $x = -20$ to $x = +20$ with steps equal to 1; c: from $x = -15$ to $x = +15$ with steps equal to 1) while the other states initial conditions are kept to 0.

more interestingly, a transition from a chaotic dissipative system to a chaotic conservative system are identified and discussed in [8]. A class of chaotic system with cyclic symmetry, which has dissipative nature, is studied and shown that interesting properties such as multistability and coexisting attractors are observed [21]. A family of chaotic systems with conservative nature is formulated and investigated for special properties in [7]. The cyclic symmetric system's intricate dynamical properties make it more suitable for various applications such as chaos-based secure communication. Their simple configuration also tackles challenges in hardware implementation. FPGA implementation of the conservative and dissipative cyclic symmetric system was carried out in [21,7].

Chaotic systems that exhibit a countable number of infinite coexisting attractors (nested) are characterized as Megastable oscillators [11–13]. A sinusoidally-driven conservative and dissipative system with signum nonlinearity is investigated for special properties and reported the existence of megastability [15]. A simple 2D chaotic system with trigonometric functions is formulated and shown the existence of countable infinite number of coexisting attractors in [16,17]. A nonlinear oscillator with an infinite number of coexisting self-excited and hidden attractors was reported in [9].

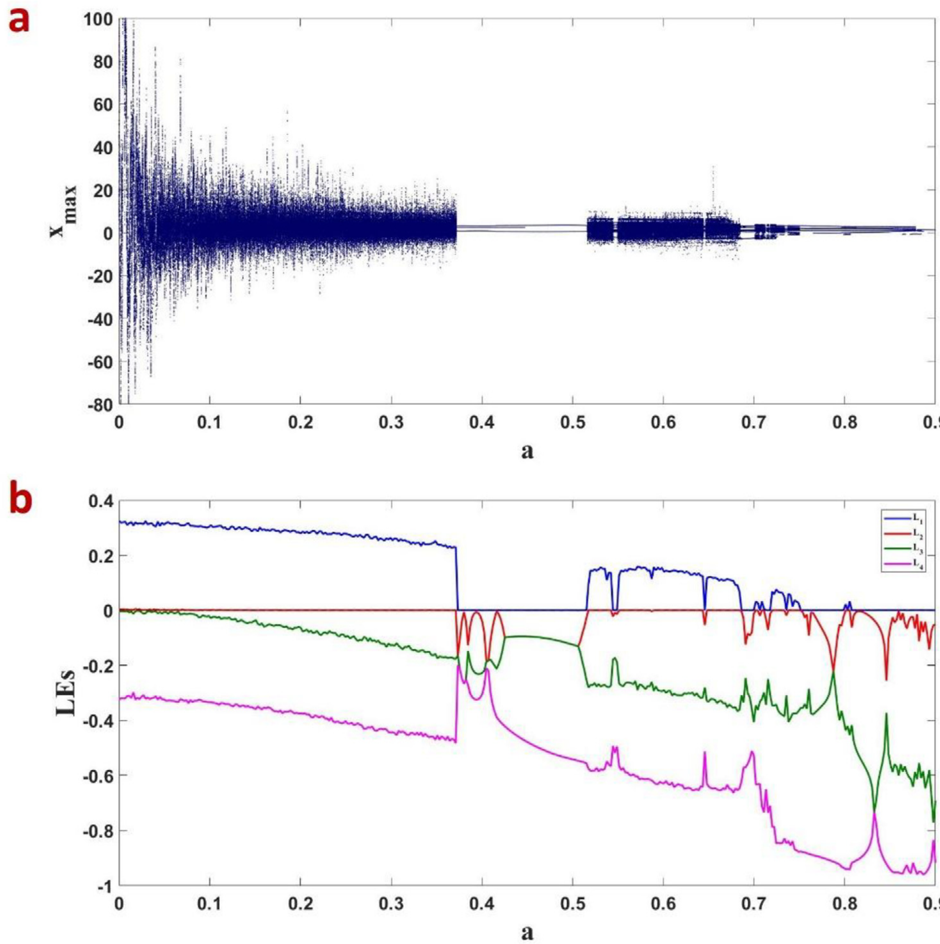

Fig. 2. Bifurcation diagram (a) and the corresponding LEs (b) of the CMO-2 system.

In the last decade, chaotic systems are mostly used in secure communication compared with other applications. Many applications are shown in this field, like masking of a message signal [22–25], encryption and decryption [26–28], information theory: random number generation [29,30], etc. Another interesting application of chaotic systems is the detection of a feeble signal. Limited numbers of papers are available on the detection of a feeble signal [27,31–38]. Most of these papers used chaotic systems for this purpose. Motivated by this finding of the literature, in this paper, an application of the proposed circulant megastable system is presented for the detection of a feeble signal.

In recent years, many optimization methods have been developed by taking inspiration from living and non-living beings; these methods are used to solve problems that are difficult to solve in real life. These inspired algorithms are developed by mimicking the behaviors of living things such as hunting, finding food, mating, and non-living things such as an explosion, spreading, gravitational force, or mathematical backgrounds [39–43]. Many algorithms have been developed in the literature to solve constraint and unconstraint optimization problems with these algorithms, generally called meta-heuristic algorithms. In several areas, including engineering, business, and research, meta-heuristic algorithms are used in solving optimization problems. In optimization problems, the main purpose of the solution process is to reduce or optimize the parameters of performance, duration, efficiency, and productivity [39]. In this study, the sine-cosine algorithm, one of the metaheuristic algorithms, was used to enhance its performance using the proposed circulant megastable system and it was used to tune the PID controller for the time-delay system concerning objective function.

A new chaotic system with an infinite number of equilibrium points is proposed and its applications are given. Specifically, in Section 1, some general information and available researches are introduced. Circulant Megastable Oscillators (CMOs) are presented in Section 2. In Section 3, a subset of chaotic systems is investigated with regard to Lyapunov exponents with the variation of some of their parameters. In Section 4, the SCA algorithm is presented and an outline of control of a time-delay system with regard to an optimization application is illustrated. In Section 5, a new improved chaotic SCA algorithm is proposed. Subsequently, in Section 6, the simulation results of the proposed chaotic SCA algorithm for solving some benchmark problems and their control applications are given. Moreover, some discussion and comparison are made. Finally, in Section 7, the conclusion of the work is drawn.

2. Circulant megastable oscillators (CMOs)

Recent literature has proposed new chaotic systems with lattices of attractors having an infinite number of equilibrium points [11–13] and some of them are unique with the countable number of coexisting attractors, named as "Megastable" after [10]. Such megastable oscillators are all chaotic Jerk systems [14–17]. Hence, we are interested in proposing a new class of chaotic oscillators that are megastable with cyclic symmetry, commonly called circu-

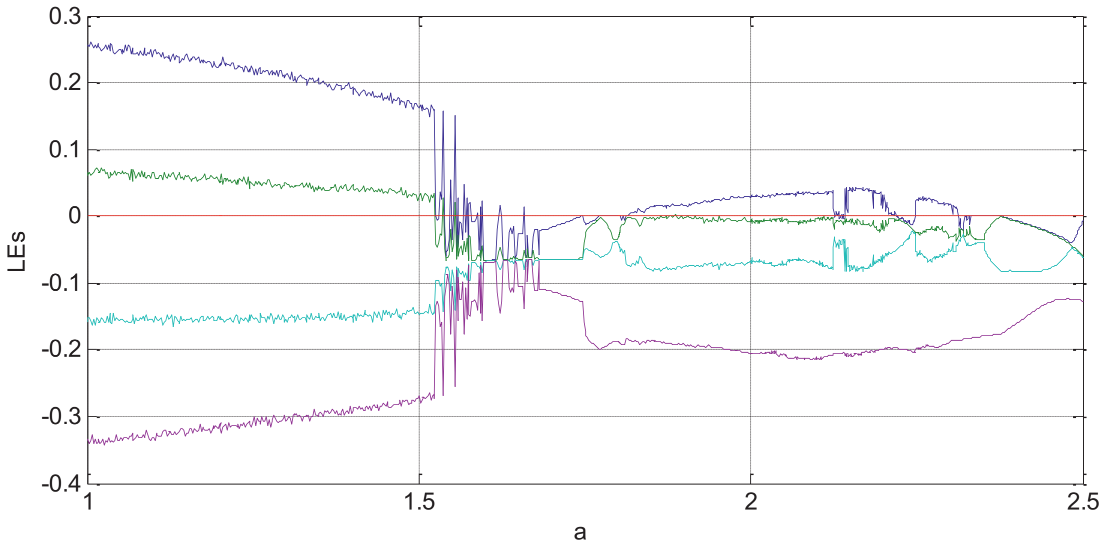

Fig. 3. Lyapunov spectrum with the variation of parameter a keeping other parameters fixed at $b = 0.2,\ \omega = 1$ of the CMO-3 system.

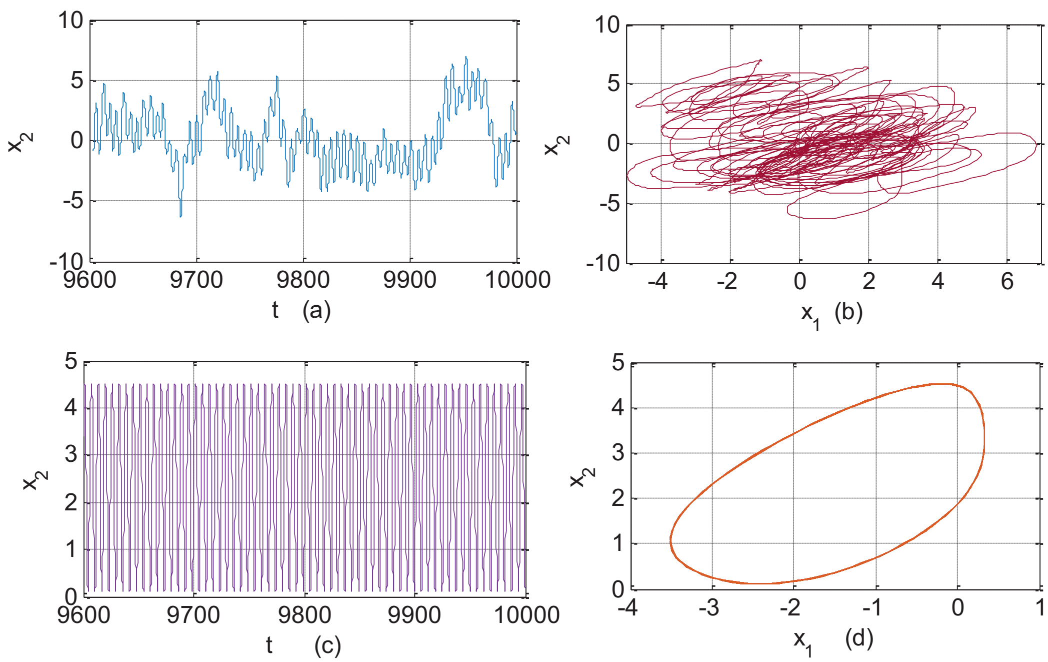

Fig. 4. Behavior of the CMO-3 system with $b = 0.2,\ \omega = 1,\ \omega_0 = 10,\ x(0) = (0.1, 0.1,\ 0,\ 0,\ 0)^T$ for: (a), (b) $a = 1.525000217$; chaotic behavior and (c), (d) with the addition of a feeble signal of amplitude $A = 10^{-9}$.

lant systems [18,19–21]. Table 1 shows a class of circulant systems showing cyclic symmetry.

The phase portraits of the CMO systems for different initial conditions $(x,\ 0,\ 0)$ are shown in Fig. 1. The value of x is chosen from a selected range and a step size. It should be noted that all the attractors shown in Fig. 1 (with different colors) are chaotic and never disintegrates to a tori as in many other cases of megastable oscillators [5–8].

In the subsequent investigation, we consider the bifurcation of the CMO-2 with parameter a. The system shows chaotic attractors for about $0<a \le 0.38$ and $0.52 \le a \le 0.7$, as shown in Fig. 2a. For $0<a \le 0.9$, we could see chaotic regions and the same can be confirmed with the respective LEs plotted in Fig. 2b. Especially for about $0<a \le 0.38$ and $0.52 \le a \le 0.7$ 8, the CMO-2 system enters the chaotic region.

3. Application of CMO-3 system for detection of a feeble signal

This section describes an application of the CMO-3 system for detecting a feeble signal. The Lyapunov spectrum with the variation of parameter $a = [1,\ 2.5]$ and $b = 0.2,\ \omega = 1$, a fixed initial condition $(x(0),\ y(0),\ z(0),\ w(0), p(0)) = (0.1, 0.1,\ 0,\ 0,\ 0)$ of the CMO-3 system is shown in Fig. 3. The Lyapunov spectrum is calculated, after transforming the CMO-3 system into an autonomous form, by using Wolf et al. [18] algorithm considering total iteration time $T = 10,000$ and a step size $\Delta t = 0.02$. It is seen from Fig. 3 that the CMO-3 system has various dynamical behaviors like hyperchaotic, chaotic, quasiperiodic and periodic. For example, when $a \in\ [1,\ 1.5]$, two Lyapunov exponents are positive and hence, it confirms the hyperchaotic behavior. Again, when $a \in\ [1.9,\ 2.1]$, the presence of only one positive Lyapunov expo-

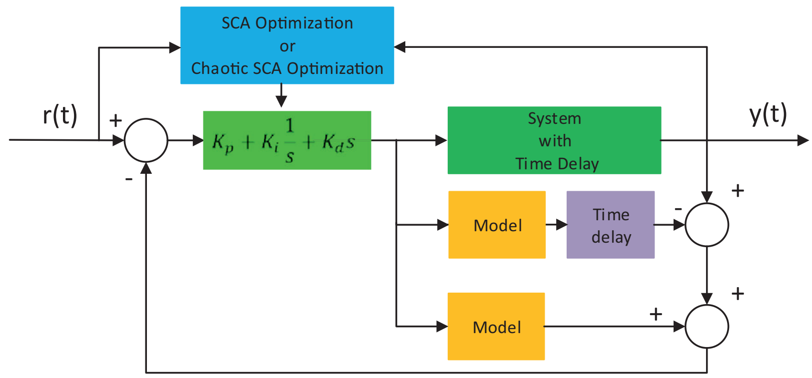

Fig. 5. Smith Predictor for PID controller using the SCA optimization or Chaotic SCA optimization algorithm. (For interpretation of the references to colour in this figure legend, the reader is referred to the web version of this article.)

nent indicates a chaotic behavior. Further, when $a \in [2.4, 2.5]$, the nature of Lyapunov exponents is (0, -, -, -, -) which suggests the presence of periodic behavior. For some value of a, Lyapunov exponents have nature as (0, 0, -, -, -) indicating the presence of quasiperiodic behavior. Fig. 3 suggests and further numerical simulation reveals that when $a = 1.525000217$, the behavior of the CMO-3 system is chaotic. However, when a is increased by a small value of the order 10^{-9}, i.e. $a = 1.525000218$, the behavior of the CMO-3 system is changed from chaotic to periodic. Therefore, it may be considered that $a_T = 1.525000217$ is the threshold value for parameter a for the CMO-3 system since it changes its behavior from chaotic nature to periodic nature with an addition of a feeble signal of the form $10^{-9}\sin(\omega_0\tau)$. Thus, the CMO-3 system can be used for generating an alarm for detecting a feeble signal.

CMO-3 system with the state variables $x_1 = x,\ x_2 = y,\ x_3 = z, x_4 = w$ is written in (1).

$$\begin{aligned}\dot{x}_1 &= \cos(x_2) - b\tanh(x_1) - a\sin(\omega t)\\ \dot{x}_2 &= \cos(x_3) - b\tanh(x_2) - a\sin(\omega t)\\ \dot{x}_3 &= \cos(x_4) - b\tanh(x_3) - a\sin(\omega t)\\ \dot{x}_4 &= \cos(x_1) - b\tanh(x_4) - a\sin(\omega t)\end{aligned} \tag{1}$$

The application of the CMO-3 system in (1) for detecting a feeble signal can be achieved by considering $t = \omega_0\tau$, where ω_0 is the frequency of the feeble signal. The CMO-3 system can be written as in (2).

$$\begin{aligned}\dot{x}_1 &= \omega_0(\cos(x_2) - b\tanh(x_1) - a\sin(\omega\omega_0\tau))\\ \dot{x}_2 &= \omega_0(\cos(x_3) - b\tanh(x_2) - a\sin(\omega\omega_0\tau))\\ \dot{x}_3 &= \omega_0(\cos(x_4) - b\tanh(x_3) - a\sin(\omega\omega_0\tau))\\ \dot{x}_4 &= \omega_0(\cos(x_1) - b\tanh(x_4) - a\sin(\omega\omega_0\tau))\end{aligned} \tag{2}$$

Here, to detect a feeble signal using the CMO-3 system, an input u consists of the feeble signal is added. The system in (2) is rewritten as

$$\begin{aligned}\dot{x}_1 &= \omega_0(\cos(x_2) - b\tanh(x_1) - a\sin(\omega\omega_0\tau))\\ \dot{x}_2 &= \omega_0(\cos(x_3) - b\tanh(x_2) - a\sin(\omega\omega_0\tau))\\ \dot{x}_3 &= \omega_0(\cos(x_4) - b\tanh(x_3) - a\sin(\omega\omega_0\tau))\\ \dot{x}_4 &= \omega_0(\cos(x_1) - b\tanh(x_4) - a\sin(\omega\omega_0\tau) + u)\end{aligned} \tag{3}$$

where $u = A\sin(\omega_0\tau)$ is a feeble signal; A is the amplitude and τ change in time scale. It is observed from the simulation results that the CMO-3 system can detect a feeble signal of very high frequency.

The nature of the CMO-3 system with $a = 1.525000217$ and after the addition of a feeble signal of amplitude $A = 10^{-9}$ is shown, respectively, in Fig. 4(a),(b) and (c),(d). It is seen from Fig. 4(a), (b) that the system has chaotic behavior. It is apparent from Fig. 4(c), (d) that the CMO-3 system has periodic behavior with the addition of the feeble signal of amplitude $A = 10^{-9}$. Thus, a feeble signal of the order 10^{-9} is detected using the CMO-3 system.

4. The controller designer by using sca algorithm

The Sine-Cosine Algorithm (SCA), controller design, and newly developed chaotic SCA are explained in this section. After that, the PID controller is designed using this algorithm for a time-delay system.

4.1. SCA algorithm

The SCA algorithm is a swarm intelligence based optimization algorithm proposed by Mirjalili in 2016 [43]. Many researchers have examined this algorithm for its simplicity, applicability, low parameter content, and developability. It has been studied in support-vector optimization, short-term hydrothermal parameter scheduling, and many engineering fields. This swarm-based algorithm is updated using (4), as proposed by Mirjali, for each individual in the swarm. A pseudocode of the general algorithm is given in Algorithm 1. In Algorithm 1, t represents the current iteration, X_{best} presents at the current iteration, $X_{best,j}$ is the jth dimension value of the optimal individual, $X_{i,j}$ is the jth dimension value of the individual i at iteration t and $r_1, r_2,\ r_3,\ and\ r_4$ are random variables. The random variables r_1 (Eq. (5)) and r_3 have a uniform distribution between 0 and 2; r_2 has a uniform distribution between 0 and 2π; r_4 has a uniform distribution between 0 and 1 [43].

$$X_{i,j} \leftarrow \begin{cases} X_{i,j} + \left(r_1 \times\ \sin(r_2)\ \times \left|r_3 \times X_{best,j} - X_{i,j}\right|\right) & 0 \le r_4 < 0.5 \\ X_{i,j} + \left(r_1 \times\ \cos(r_2)\ \times \left|r_3 \times X_{best,j} - X_{i,j}\right|\right) & 0.5 \le r_4 < 1 \end{cases} \tag{4}$$

$$r_1 = \alpha\left(1 - \frac{t}{T}\right) \tag{5}$$

4.2. Controller design

Time-delay systems are the most common systems in the industry. Due to such structure, when a signal is applied to the system, the output can be observed at the exit of the system after a certain time [44,45]. A conventional PI or PID controller may be used to control such systems. But when PI or PID controllers are applied, the system may respond slowly. In addition, the control signal may not be suitable for time-delay systems due to the derivative operator of PID controllers. Thus, the smith predictor is proposed that enables the application of the control signal by taking into account the dead time of the system. The Smith predictor based controller can compensate the dead time effectively for controlling large time-delay systems. Such structure predicts the time-delay and applies a control signal to the system accordingly [45].

Algorithm 1
Pseudocode of the SCA algorithm.

Result: Pseudo-code of SCA algorithm
Initialize the random population X_i $[i = 1, 2, ..., N]$
Calculate the fitness values for each $F(X_i)$ and find the best $F(X_{best})$
for t=1:N_{iter} **do**
  $r_1 \leftarrow a \times (1 - t/N_{iter})$
  for i=1:N **do**
    for j=1:N **do**
      $r_2 \leftarrow (2 \times \pi) \times rand()$
      $r_3 \leftarrow 2 \times rand()$
      $r_4 \leftarrow rand()$
      if $r_4 < 0.5$ **then**
        $X_{i,j} \leftarrow X_{i,j} + (r_1 \times sin(r_2) \times |r_3 \times X_{best,j} - X_{i,j}|$
      else
        $X_{i,j} \leftarrow X_{i,j} + (r_1 \times cos(r_2) \times |r_3 \times X_{best,j} - X_{i,j}|$
      end
    end
  end
  for i=1:N **do**
    if $F(X^i) < F(X_{best})$ **then**
      $X^{best} \leftarrow X_i$
    end
  end
end

Algorithm 2
Pseudocode of the Chaotic SCA algorithm.

Result: Pseudo-code of CMO-k-SCA algorithm
Initialize the random population X_i $[i = 1, 2, ..., N]$
Calculate the fitness values for each $F(X_i)$ and find the best $F(X_{best})$
$n \leftarrow 0$
for t=1:N_{iter} **do**
  $r_1 \leftarrow a \times (1 - \frac{t}{N_{iter}})$
  for i=1:N **do**
    for j=1:N **do**
      $r_2 \leftarrow (2 \times \pi) \times rand()$
      $r_3 \leftarrow 2 \times rand()$
      $r_4 \leftarrow rand()$
      $n \leftarrow n + 0.001$
      if $r_4 < 0.475$ **then**
        $X_{i,j} \leftarrow X_{i,j} + (r_1 \times sin(r_2) \times |r_3 \times X_{best,j} - X_{i,j}|$
      else if $r_4 < 0.95$ **then**
        $X_{i,j} \leftarrow X_{i,j} + (r_1 \times cos(r_2) \times |r_3 \times X_{best,j} - X_{i,j}|$
      else
        $X_{i,j} \leftarrow X_{i,j} + (\mathrm{x_k(n)} \times \frac{2}{1+e^{X_{best,j}-X_{i,j}}} \times (X_{best,j} - X_{i,j})$
      end
    end
  end
  for i=1:N **do**
    if $F(X^i) < F(X_{best})$ **then**
      $X^{best} = X_i$
    end
  end
end

Smith predictor used to control time-delay systems separates the system's dead-time part from the time-delay model of the system. After that, using the model, a controller is designed for the system and adapted to the designed controlled system to apply the control signal. Poorani et al. made a comparison between classical PID and Smith predictor for heat exchanger. They concluded that the performance is better when the Smith predictor was used [46]. On the other hand, Yücelen designed a PI controller for the Smith predictor to control a thermal system [47]. Gurban et al. proposed a modified Smith predictor for greenhouse gas control using a genetic algorithm to determine its parameters [48]. In this study, using the approach given in Fig. 5, a controller was designed and implemented for the time-delay system. The parameters of the controller were determined so that the performance criteria in Eq. (6) are met.

$$\begin{aligned} \min\,(J(u)) &= \int_0^{tf} (r(t) - y(t))^2 \\ u_{min} &\le u \le u_{max} \end{aligned} \tag{6}$$

5. Improved chaotic sca algorithm

In this study, a chaotic SCA algorithm is proposed by adding chaotic behavior in the SCA algorithm. The process was carried out by modifying Eq. (4), used in the SCA algorithm, and proposing a new Eq. (7). The chaotic SCA algorithm is developed by using the state $(x_k(t))$ of the CMO-3 system in Eq. (7). The CMO-3 chaotic system has four states; thus, four chaotic SCA algorithms were developed by changing the index k, and named as Chaotic-1-SCA,

Table 2
Results of the SCA, Chaotic-1-SCA, Chaotic-2-SCA, Chaotic-3-SCA, Chaotic-4-SCA Algorithms for the benchmark problems.

Function Number	SCA		Chaotic-1-SCA		Chaotic-2-SCA		Chaotic-3-SCA16		Chaotic-4-SCA	
	Average	Standard Deviation	Average	Standard Deviation	Average	Standard Deviation	Average	Standard Deviation	Average	Standard Deviation
1	1,93E-35	1,03E-34	2,14E-42	7,62E-42	**3,63E-43**	2,16E-42	1,15E-42	4,02E-42	3,68E-40	1,53E-39
2	4,26E-24	1,23E-23	1,16E-27	2,71E-27	**2,21E-28**	1,14E-27	6,04E-28	1,80E-27	8,93E-27	2,10E-26
3	1,88E-15	9,36E-15	1,50E-19	6,95E-19	**2,87E-20**	1,85E-19	2,26E-19	1,29E-18	6,17E-18	4,31E-17
4	1,30E-12	5,35E-12	8,00E-15	1,78E-14	**8,12E-16**	1,56E-15	5,79E-14	2,85E-13	1,63E-14	4,03E-14
5	6,685,837	0,398,765	6,341,763	0,5372	**6,316,113**	0,348,167	6,370,454	0,542,247	6,50,724	0,446,197
6	0,209,754	0,122,717	0,1185	0,112,371	**0,106,031**	0,13,942	0,120,675	0,137,199	0,116,062	0,119,015
7	0,000,285	0,000,251	0,000,222	0,000,227	**0,000,138**	0,000,193	0,00,023	0,000,226	0,000,228	0,000,181
8	−2436,63	166,3504	**−2450,26**	207,2559	−2354,15	136,5909	−2399,53	153,032	−2391,14	176,9144
9	0,001,211	0,008,564	**0**	**0**	6,01E-10	4,25E-09	**0**	**0**	3,05E-09	2,15E-08
10	4,09E-15	1,08E-15	3,80E-15	1,38E-15	**3,73E-15**	1,44E-15	3,87E-15	1,32E-15	4,01E-15	1,17E-15
11	0,021,861	0,098,783	0,004,081	0,028,848	0,029,999	0,092,246	**0,004,031**	0,028,503	0,013,038	0,060,344
12	0,048,512	0,023,338	0,033,687	0,015,756	**0,023,141**	0,015,651	0,033,961	0,016,385	0,037,373	0,014,767
13	0,176,767	0,06,915	0,140,329	0,082,588	**0,105,178**	0,074,279	0,136,651	0,083,357	0,137,163	0,092,785
14	1,196,422	0,601,271	**1,037,688**	0,280,594	1,07,738	0,392,748	1,196,419	0,601,272	1,037,689	0,280,594
15	0,000,902	0,000,425	0,000,851	0,000,435	0,000,814	0,00,043	**0,000,655**	0,000,404	0,000,794	0,000,427
16	**−1,03,163**	8,63E-06	**−1,03,163**	1,55E-06	**−1,03,163**	9,74E-07	**−1,03,163**	1,78E-06	**−1,03,163**	**1,05E-06**
17	0,398,175	0,000,277	**0,398,043**	0,000,155	0,398,081	0,000,252	0,39,817	0,000,411	0,398,055	0,000,206
18	**3,000,001**	1,53E-06	**3,000,001**	1,75E-06	**3,000,001**	**6,69E-07**	**3,000,001**	1,93E-06	**3,000,001**	1,39E-06
19	−3,85,593	0,002,764	−3,85,647	0,003,185	−3,85,669	0,003,328	**−3,85,621**	**0,003,016**	−3,85,647	0,00,316
20	−3,03,877	0,14,813	−3,03,793	0,148,659	**−3,08,097**	0,212,638	−3,08,001	0,114,223	−3,0468	0,158,625
21	−3,90,746	2,065,115	−4,62,658	2,009,237	−5,06,009	2,440,151	**−5,61,868**	1,914,109	−5,06,178	2,005,741
22	−5,35,215	1,652,579	−5,72,598	2,109,694	**−6,18,719**	2,18,923	−5,91,893	2,06,242	−5,97,907	1,648,619
23	−5,5916	1,516,255	−6,61,928	1,818,378	−6,47,994	1,940,142	**−6,72,181**	1,740,799	−5,93,268	1,578,227

Chaotic-2-SCA, Chaotic-3-SCA, and Chaotic-4-SCA. Therefore, it is aimed to increase both the global and local search performance of the algorithm developed by hybridizing with chaotic behavior. To realize this, a very small probability is added to the algorithm, adding to this chaotic behavior and a behavior multiplied by a sigmoid-like function to limit the situation. This behavior added to the SCA algorithm with probability of 0.05 is realized using Eq. (7). The pseudocode of the Chaotic SCA algorithm is given in Algorithm 2.

$$X_{i,j} \leftarrow \begin{cases} X_{i,j} + \left(r_1 \times \sin(r_2) \times \left|r_3 \times X_{best,j} - X_{i,j}\right|\right) & 0 \le r_4 < 0.475 \\ X_{i,j} + \left(r_1 \times \cos(r_2) \times \left|r_3 \times X_{best,j} - X_{i,j}\right|\right) & 0.475 \le r_4 < 0.95 \\ X_{i,j} + \left(x_k(t) \times \frac{2}{1+e^{X_{best,j}-X_{i,j}}} \left|X_{best,j} - X_{i,j}\right|\right) & 0.95 \le r_4 < 1 \end{cases} \tag{7}$$

6. Simulation results

In this study, 23 benchmark problems, which are widely used in the literature [41–43], are selected to compare the developed Chaotic SCA algorithms' performance. These are unimodal, multimodal, and fixed-dimension multimodal benchmark problems. These benchmark problems have been tested, and the statistical results are presented graphically and in tables. Then, the proposed new algorithms' performance is tested on the controller design problem to control the time-delay systems. The algorithms' swarm size was considered as 100 and the number of iterations as 500 to test the proposed algorithms. Besides, each algorithm was run independently 20 times on the same problem and technique for equitable comparison in the statical analysis. These results were obtained using a computer with Intel (R) Core (TM) i7–6700 HQ CPU @ 2.60 GHz, 64 Bit, 8GB RAM. The study was carried out using the MATLAB 2018a program. The abbreviations of the developed algorithms have been made in a simple manner and these abbreviations are used in tables and graphics. Simulation results are given in Table 2. Also, graphical results are shown in Figs. 6–8.

The average value and the standard deviation of all the 23 benchmark problems are calculated using the four Chaotic SCA algorithms and presented in Table 2. In Figs. 6–8, the global minimum value, average value, and maximum values of the four algorithms are shown. The results suggest that the estimated average values and the minimum values by the algorithms are not always the same. For better visualization, the best minimum, average and maximum values among the 20 experiments data were plotted in Figs. 6–8. The global minimum values of these functions are given in [41-42], and the global minimum value found by the algorithms will be accepted as the smallest value of a problem.

From Table 2 and Figs. 6–8, we observe that the best global minimum is obtained by Chaotic-1-SCA algorithm for the functions F5, F8, F9, F16; Chaotic-2-SCA algorithm for F2, F6, F11, F12, F18, F20; Chaotic-3-SCA algorithm for F3, F15, F19, F21, F23 and Chaotic-4-SCA algorithm for F7, F22. However, all four algorithms perform equally for F10, F11, F14 and F17.

Further, we observe from Table 2 and Figs. 6–8 that the best average value is obtained by using Chaotic-1-SCA for the functions F8, F14, F17; Chaotic-3-SCA for F9, F11, F15, F19, F21, F-23; only F16 is the best optimized using Chaotic-4-SCA and the rest all functions have shown their best average value performance using Chaotic-2-SCA algorithm.

Two time-delay systems are considered to check the performance of the controller. These are given in Eqs. (8) and (9).

$$G_1 = \frac{1}{s+1} e^{-s} \tag{8}$$

$$G_2 = \frac{1}{(s+1)^2} e^{-0.5s} \tag{9}$$

We have considered different PID controllers available for the G_1 system from the literature for comparing the performance with the proposed controllers. The controller parameters and value of the objective function are given in Table 3. From Table 3, it is found that the Chaotic-3-SCA algorithm has resulted the optimal controller parameters and exhibits the global minimum value for this system. The responses of the G_1 system by all the controllers in Table 3 and their corresponding control signals are shown in Fig. 9. It can be concluded from Fig. 9 that the performance of the G_1 system is comparatively better by using the proposed Chaotic-3-SCA algorithm.

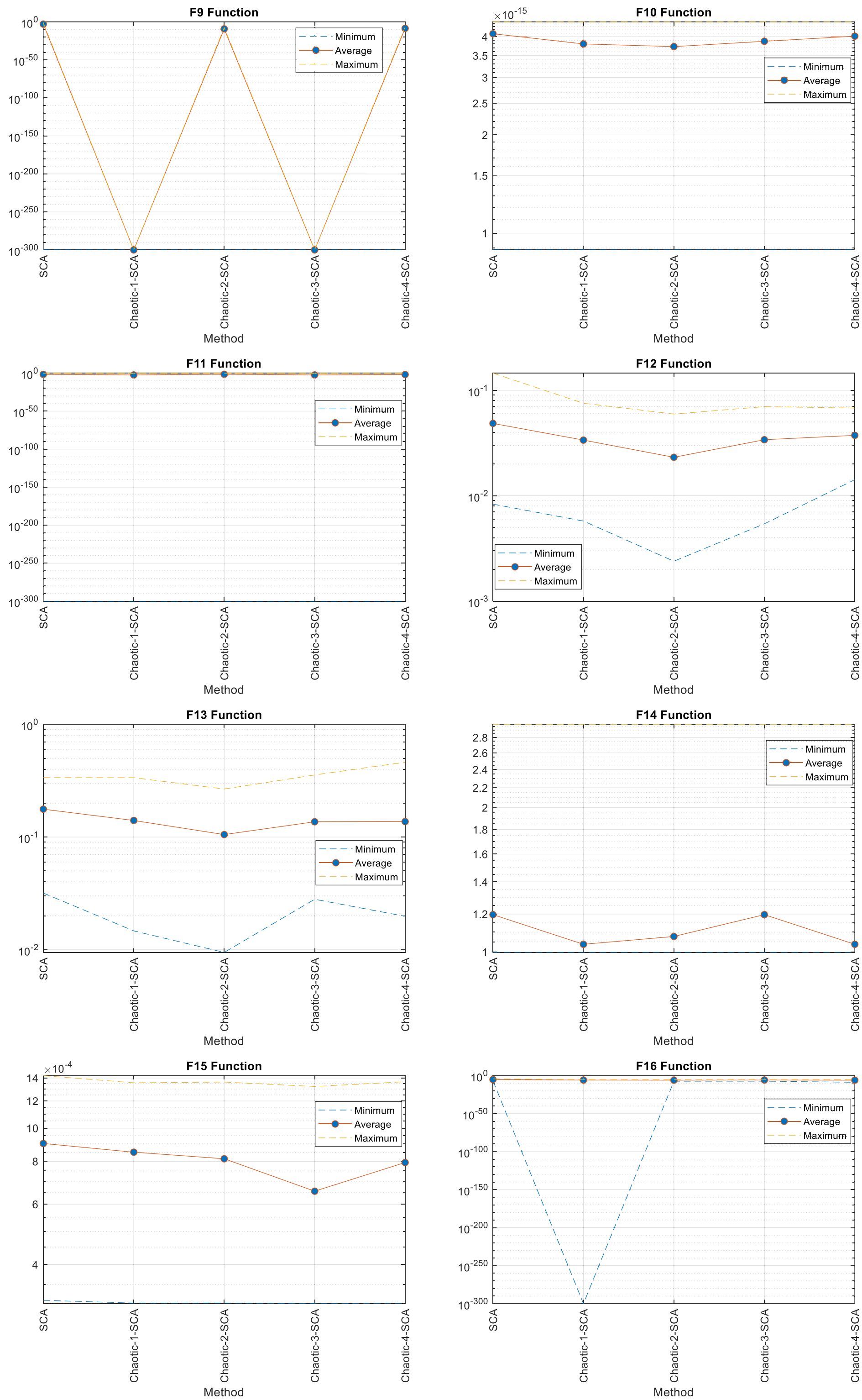

Fig. 6. Minimum, average and maximum results of F1-F8 functions using SCA, Chaotic-1-SCA, Chaotic-2-SCA, Chaotic-3-SCA and Chaotic-4-SCA.

A similar approach is used for the G_2 system also. Various controllers, their parameters and the value of the objective function for the G_2 system are given in Table 4. When Table 4 is examined, the performance of the Chaotic-2-SCA algorithm is observed to have resulted in the optimal controller parameters, which result in the global minimum value of the objective function. Fig. 10 displays the responses by using different controllers of the G_2 system and their corresponding control signals. Therefore, the comparatively better performance of the G_2 system is observed when

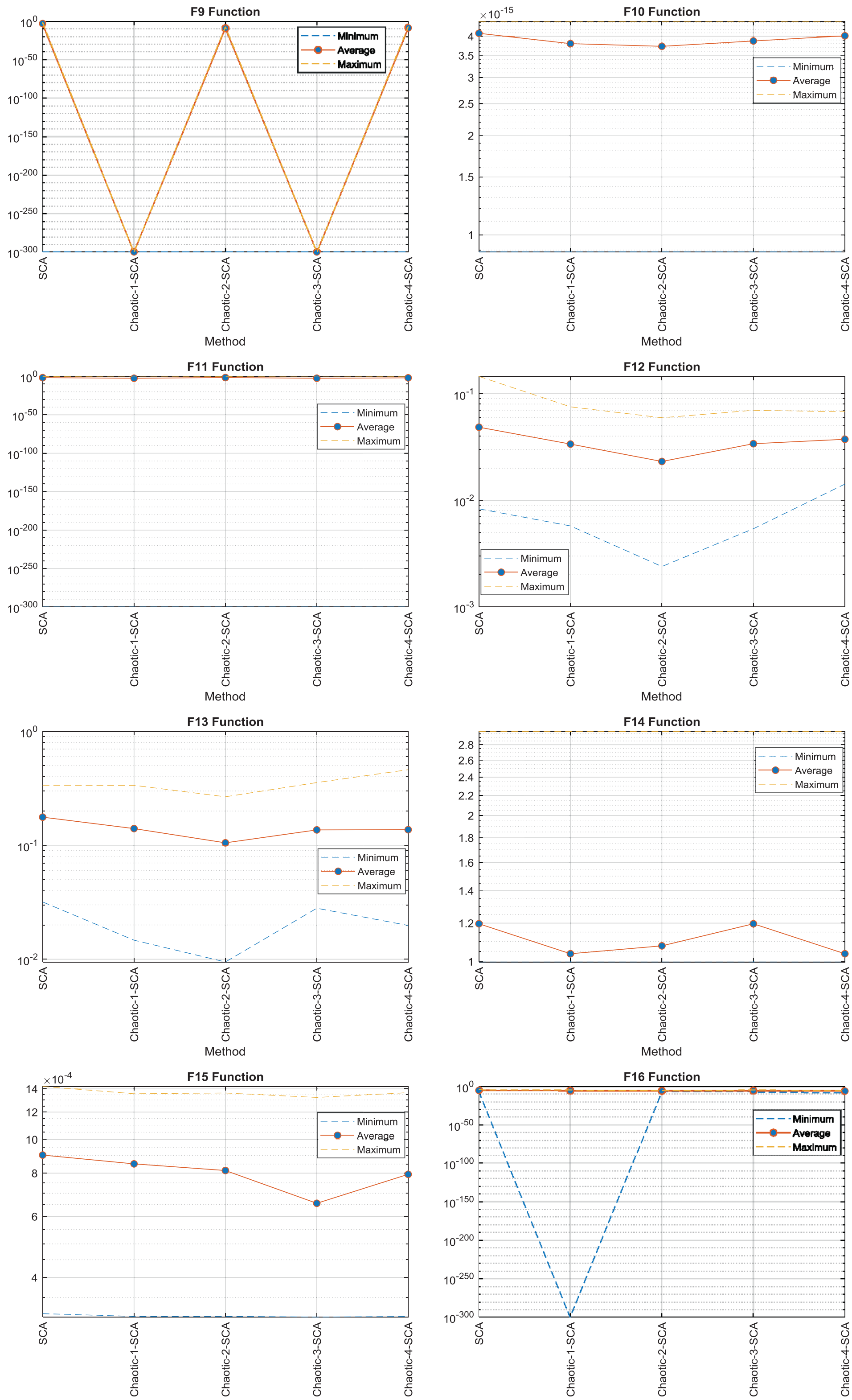

Fig. 7. Minimum, average and maximum results of F9-F16 functions using SCA, Chaotic-1-SCA, Chaotic-2-SCA, Chaotic-3-SCA, and Chaotic-4-SCA.

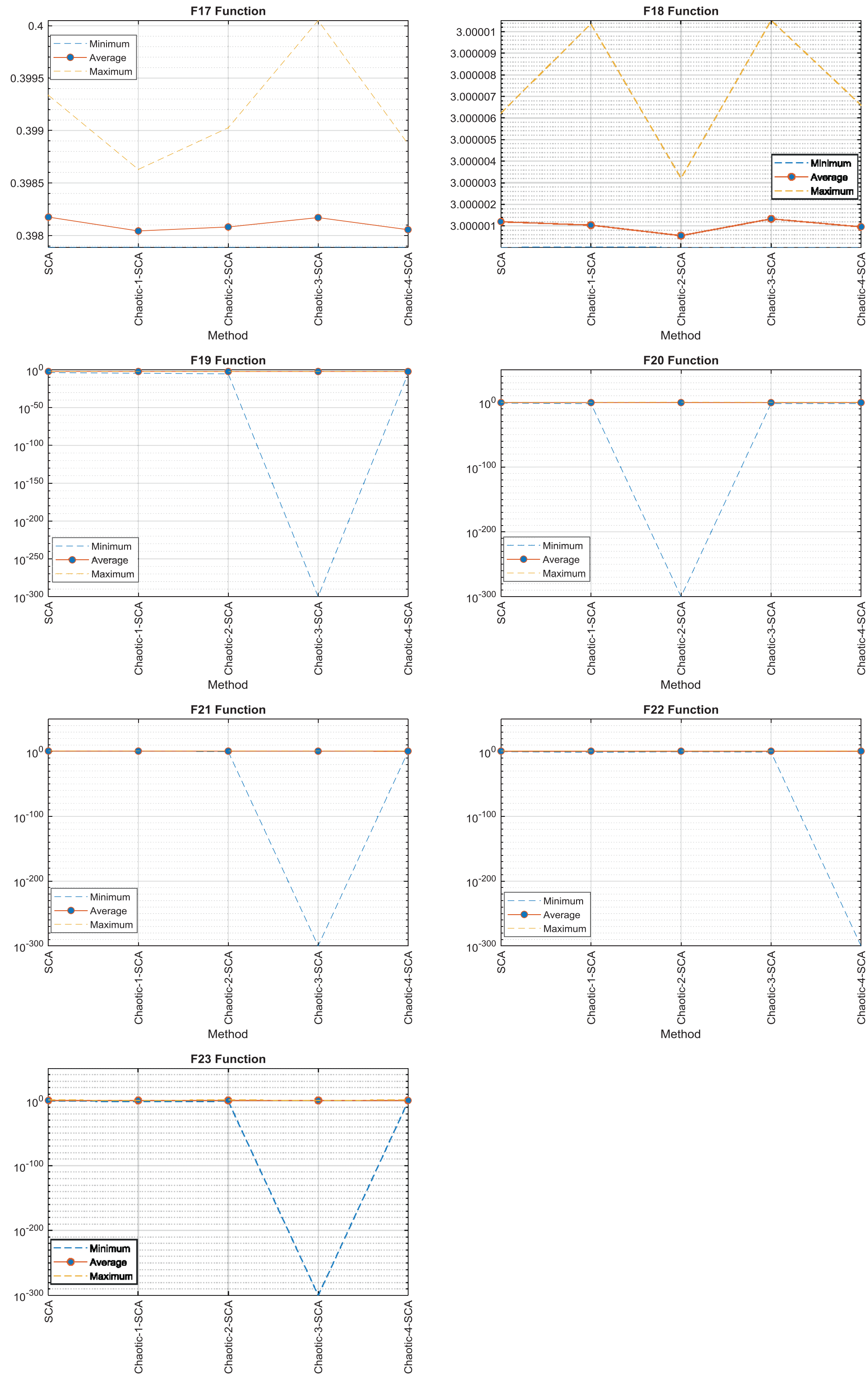

Fig. 8. Minimum, average and maximum results of F17-F23 functions using SCA, Chaotic-1-SCA, Chaotic-2-SCA, Chaotic-3-SCA, and Chaotic-4-SCA.

Table 3
Results of SCA, Chaotic-1-SCA, Chaotic-2-SCA, Chaotic-3-SCA, Chaotic-4-SCA Algorithms for G_1 system.

	K	Ki	Kd	J
PID zeigler Nichols Step response [44]	1.206	0.6029	0.6026	0.518004971868672
PID zeigler Nichols frequency response [44]	1.315	0.8766	0.5197	0.389124898449892
PID AMIGO Step response [44]	0.6562	0.5966	0.252	0.747419584344242
PID AMIGO frequency response [44]	0.6726	0.6794	0.2959	0.670936749971241
WAO PID [44]	3	6.4208	3.7142e-20	0.144467979068028
SCA PID	2.97985124535648	10	1.0000e-200	0.138196119928278
Chaotic-1-SCA PID	2.98012964766160	10	3.4933e-200	0.138186453379259
Chaotic-2-SCA PID	2.97792806098344	10	1.0000e-200	0.138262932755003
Chaotic-3-SCA PID	2.98498675950492	9.94883762221232	1.1517e-200	**0.138082548480609**
Chaotic-4-SCA PID	2.98490193270897	9.94007446673270	1.6112e-199	0.138096606470739

Table 4
Results of SCA, Chaotic-1-SCA, Chaotic-2-SCA, Chaotic-3-SCA, Chaotic-4-SCA algorithms for the G_2 system.

	K	Ki	Kd	J
PID zeigler Nichols Step response [44]	0.9895	0.2151	1.138	0.830028847831779
PID zeigler Nichols frequency response [44]	1.058	0.2859	1.247	0.725802624889884
PID AMIGO Step response [44]	0.5641	0.2565	0.5026	1.185951331817125
PID AMIGO frequency response [44]	0.4943	0.2472	0.4844	1.115631284054570
WAO PID [44]	2.9592	0.9953	1.1633e-20	0.575511287475820
SCA PID	2.9153	1.1938	1.0229e-200	0.571781805682726
Chaotic-1-SCA PID	2.9224	1.1732	1.8621e-200	0.571520341305722
Chaotic-2-SCA PID	2.9205	1.1875	1.7946e-200	**0.571390614763884**
Chaotic-3-SCA PID	2.9146	1.2189	1.5324e-200	0.571392803613831
Chaotic-4-SCA PID	2.9124	1.2254	1.0000e-200	0.571524734649332

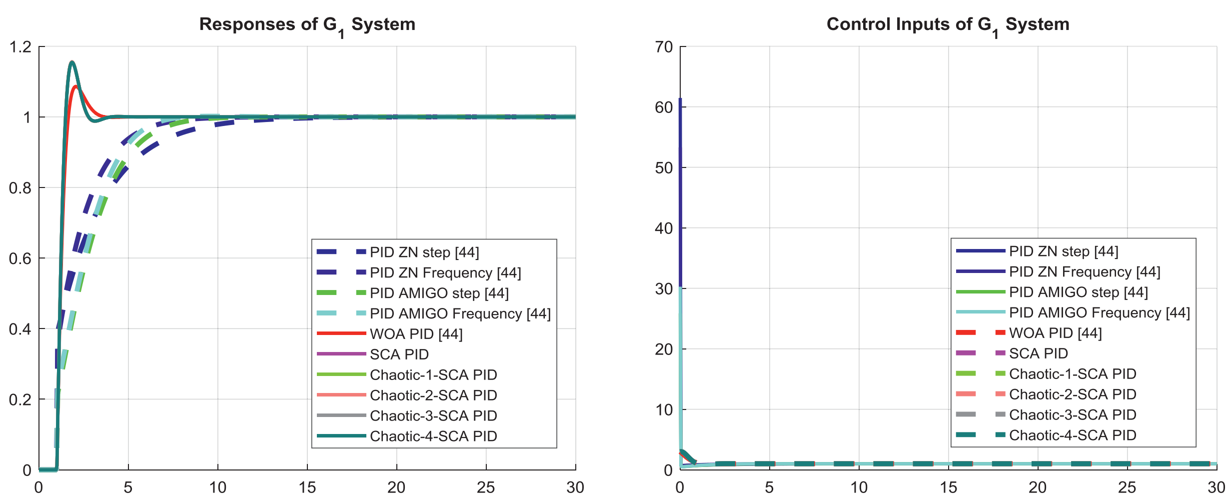

Fig. 9. (a) System response and (b) control signal for the G_1 system.

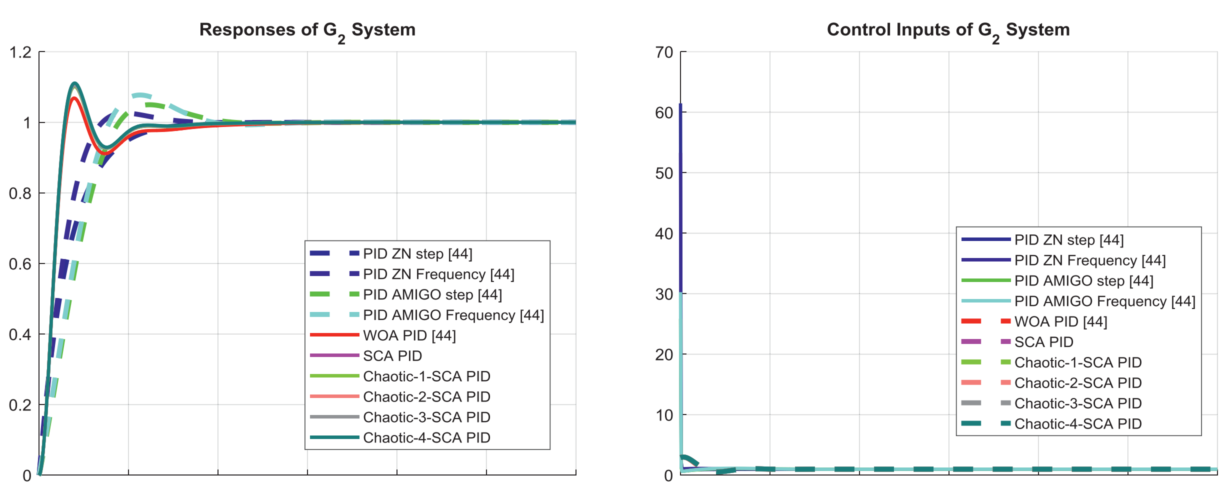

Fig. 10. (a) System response and (b) control signal for the G_2 system.

Table 5
Performance Comparison of SCA, Chaotic-1-SCA, Chaotic-2-SCA, Chaotic-3-SCA, Chaotic-4-SCA algorithms for the systems G_1 and G_2.

System Number	SCA		Chaotic-1-SCA		Chaotic-2-SCA		Chaotic-3-SCA		Chaotic-4-SCA	
	Average	Standard Deviation	Average	Standard Deviation	Average	Standard Deviation	Average	Standard Deviation	Average	Standard Deviation
1	0.1386	0.0007	0.1383	0.0003	**0.1383**	**0.0002**	**0.1383**	**0.0002**	**0.1383**	**0.0002**
2	0.5748	0.0032	0.5752	0.0037	**0.5739**	**0.0020**	0.5745	0.0029	0.5744	0.0030

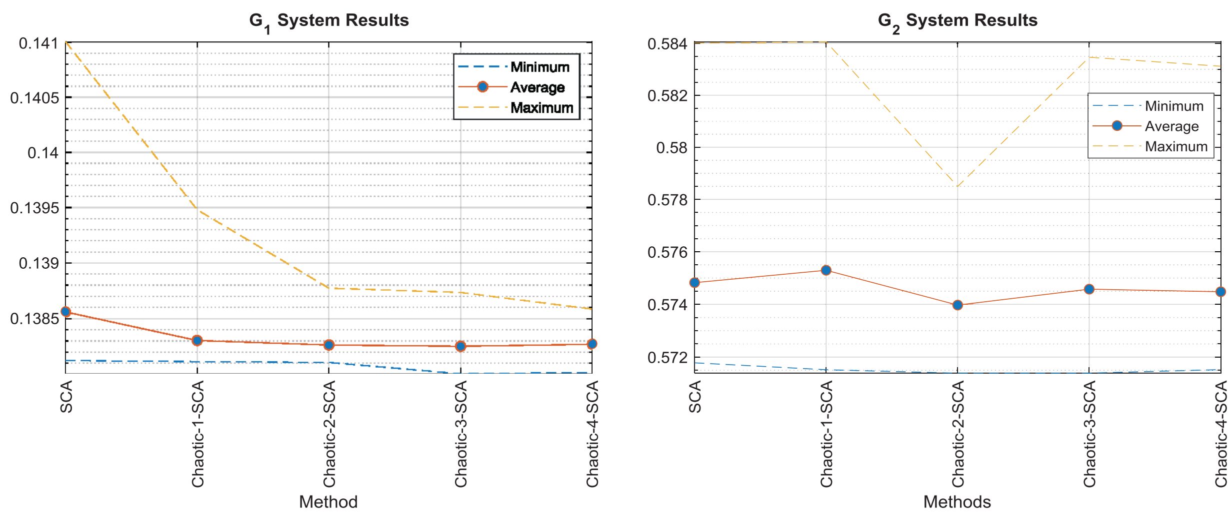

Fig. 11. Minimum, average, and maximum results of controlling of G1 and G2 using SCA, Chaotic-1-SCA, Chaotic-2-SCA, Chaotic-3-SCA, and Chaotic-4-SCA.

the system is controlled using the Chaotic-2-SCA algorithm than all other controllers considered in Table 4.

A comparative analysis of the proposed four algorithms and the basic SCA algorithm for controlling the considered systems G_1 and G_2 is given in Table 5 and shown in Fig. 11. It is observed that in terms of global minimum, the Chaotic-3-SCA algorithm has yielded the best results for the G_1 system. But in terms of average value, Chaotic-1-SCA, Chaotic-2-SCA, and Chaotic-3-SCA algorithms exhibit equally good result. Similarly, from Table 5 and Fig. 11, the Chaotic-2-SCA algorithm has yielded the best result for the G_2 system in terms of global minimum and average values. When evaluated in terms of general weight, it is observed that the proposed CMO-2-SCA algorithm is more successful than other algorithms.

7. Conclusion

As far as chaos theory is concerned, discovering systems with unexplored bihaviors are of interest. One such unexplored systems are those which show megastability and also has cyclic symmetry property. In this paper, we have proposed a class of cyclic symmetry system which shows megastability. Such systems were not discussed in the literature to the best of our knowledge. We have investigated the dynamical properties of the circulant megastable oscillators using Lyapunov exponents and bifurcation diagrams with the variation of a parameter. The proposed CMO-3 oscillator is applied for the detection of a feeble signal. The simulated results reveal that a feeble signal of the order 10^{-9} can be detected. Subsequently, using the randomness of megastable oscillators, a new chaotic sine-cosine optimization algorithm is developed. Subsequently, these new chaotic sine-cosine algorithms are used to estimate the PID controller parameters for time-delay systems. Consequently, the proposed controller using Chaotic-2-SCA performs better results than the results of some PID controllers available in the literature for the time-delay systems.

Declaration of Competing Interest

The authors declare that they have no known competing financial interests or personal relationships that could have appeared to influence the work reported in this paper.

References

[1] Field M, Golubitsky M. Symmetry in chaos. New York: Oxford University Press; 1992.
[2] Brisson G, Gartz K, McCune B, O'Brien K, Reiter C. Symmetric attractors in three-dimensional space. Chaos Solitons and Fractals 1996;7(7):1033–51.
[3] Reiter C. Chaotic attractors with the symmetry of the tetrahedron. Computer and Gr 1997;21(6):841–8.
[4] Reiter C. Attractors with the symmetry of the n-cube. Exp Math 1996;5(4):327–36.
[5] Dumont J, Heiss F, Jones K, Reiter C, Vislocky L. Chaotic attractors and evolving planar symmetry. Computer and Gr 1999;23:613–19.
[6] Wang Zhihui, Yan Shitao, Ouyang Peichang. Automatic Generation of Chaotic Attractors with Various Cyclic or Dihedral Symmetries. The Open Cybern & Syst J 2014;8:873–6.
[7] Gugapriya G, Rajagopal Karthikeyan, Karthikeyan Anitha, Lakshmi B. A family of conservative chaotic systems with cyclic symmetry. Pramana – J. Phys. 2018. doi:10.1007/s12043-019-1719-1.
[8] Sprott JC, Chlouverakis Konstantinos E. Labyrinth chaos. Int j bifurc and chaos 2007;17(06):2097–108.
[9] Tang Yan-Xia, Jalil Abdul, Khalaf M, Rajagopal Karthikeyan, Pham Viet-Thanh, Jafari Sajad, Tian Ye. A new nonlinear oscillator with infinite number of coexisting hidden and self-excited attractors. Chin. Phys. B Vol. 2018;27(4).
[10] Sprott JC, Jafari S, Khalaf AJM, Kapitaniak T. Megastability: coexistence of a countable infinity of nested attractors in a periodically-forced oscillator with spatially-periodic damping. Eur Phys J Spec Top 2017;226(9):1979–85.
[11] Li C, Sprott JC, Hu W, Xu Y. Infinite multistability in a self-reproducing chaotic system. Int J Bifur and Chaos 2017;27(10):1750160.
[12] Li C, Sprott JC, Mei Y. An infinite 2-D lattice of strange attractors. Nonlinear Dyn 2017;89(4):2629–39.
[13] Li C, Sprott JC. An infinite 3-D quasiperiodic lattice of chaotic attractors. Phys Lett A 2018;382(8):581–7.
[14] Rajagopal Karthikeyan, Singh Jay Prakash, Roy Binoy Krishna, Karthikeyan Anitha. Dissipative and conservative chaotic nature of a new quasi-periodically forced oscillator with megastability. Chin J Phys 2019;58:263–72.

[15] Prakash Pankaj, Rajagopal K, Singh JP, Roy BK. Megastability, Multistability in a Periodically Forced Conservative and Dissipative System with Signum Nonlinearity. Int J Bifurn and Chaos 2018;28(09):1830030.
[16] Prakash Pankaj, Rajagopal K, Singh JP, Roy BK. Megastability in a quasi-periodically forced system exhibiting multistability, quasiperiodic behaviour, and its analogue circuit simulation. AEU - Int J Electron and Commun 2018;92:111–15.
[17] Jahanshahi Hadi, Rajagopal Karthikeyan, Akgul Akif, Sari Naeimeh Najafizadeh, Namazi Hamidreza, Jafari Sajad. Complete analysis and engineering applications of a megastable nonlinear oscillator. Int J Nonlinear Mechanics 2018;107:126–36.
[18] Sprott JC. Elegant chaos: algebraically simple chaotic flows. World Scientific; 2010.
[19] Thomas R. Deterministic chaos seen in terms of feedback circuits: analysis, synthesis, “labyrinth chaos”. International Journal of Bifurcation and Chaos 1999;9(10):1889–905.
[20] Wolf A, Swift JB, Swinney HL, Vastano JA. Determining Lyapunov exponents from a time series. Physica D: Nonlinear Phenomena 1985;16(3):285–317.
[21] Rajagopal Karthikeyan, Panahi Shirin, Karthikeyan Anitha, Alsaedi Ahmed, Pham Viet-Thanh, Hayat Tasawar. Some New Dissipative Chaotic Systems with Cyclic Symmetry. Int J Bifur and Chaos 2018;28(13):1850164.
[22] Wu CW, Chua LO. A simple way to synchronize chaotic systems with applications to secure communication system. Int. J. Bifur Chaos 1993;03(06):1619–28.
[23] Cuomo KM, Oppenheim AV, Strogatz SH. Synchronization of Lorenz-based chaotic circuits with applications to communications. IEEE Trans. Circuits Syst. II Analog Digit. Signal Process. 1993;40(10):626–33.
[24] Yang T. A survey of chaotic secure communication systems. Int. J. Comput. Cogn. 2004;2(2):81–130.
[25] Singh JP, Roy BK. A more chaotic and easily hardware implementable new 3-D chaotic system in comparison with 50 reported systems. Nonlinear Dyn 2018;93(3):1121–48.
[26] Yang T, Wu CW, Chua LO. Cryptography based on chaotic systems. IEEE Trans. Circuit Syst. I Fundam. Theory Appl. 1997;44(5):469–72.
[27] Kocarev L, Lian S. Chaos-based cryptography, studies in computational intelligence. Heidelberg: Springer Berlin Heidelberg; 2011.
[28] Alawida M, Samsudin A, Teh JSen, Alkhawaldeh RS. A new hybrid digital chaotic system with applications in image encryption. Signal Processing 2019;160:45–58.
[29] Akgul A, Calgan H, Koyuncu I, Pehlivan I, Istanbullu A. Chaos-based engineering applications with a 3D chaotic system without equilibrium points. Nonlinear Dyn 2016;84(2):1–15.
[30] Akgul A, Moroz I, Pehlivan I, Vaidyanathan S. A new four-scroll chaotic attractor and its engineering applications. Optik (Stuttg) 2016;127(13):5491–9.
[31] Singh JP, Lochan K, Kuznetsov NV, Roy BK. Coexistence of single- and multi-scroll chaotic orbits in a single-link flexible joint robot manipulator with stable spiral and index-4 spiral repellor types of equilibria. Nonlinear Dyn 2017;90(2):1277–99.
[32] Wang G, Chen D, Lin J, Chen X. The application of chaotic oscillators to weak signal detection. Ind. Electron. IEEE … 1999;46(2):440–4.
[33] Rashtchi V, Nourazar M. FPGA implementation of a real-time weak signal detector using a duffing oscillator. Circuits, Syst. Signal Process. 2015;34(10):3101–19.
[34] Gokyildirim A, Uyaroglu Y, Pehlivan I. A novel chaotic attractor and its weak signal detection application. Optik (Stuttg) 2016;127(19):7889–95.
[35] Li-xin MA. Weak Signal Detection Based on Duffing Oscillator. In: IEEE International Conference on Information Management, Innovation Management and Industrial Engineering; 2008. p. 430–3.
[36] Li G, Zhang B. A novel weak signal detection method via chaotic synchronization using Chua’s circuit. IEEE Trans. Ind. Electron. 2017;64(3):2255–65.
[37] Luo J, Xu X, Ding Y, Yuan Y, Yang B, Sun K, Yin L. Application of a memristor-based oscillator to weak signal. Eur. Phys. J. Plus 2018;133:239.
[38] Gokyildirim A, Uyaroglu Y, Pehlivan I. A weak signal detection application based on hyperchaotic Lorenz system. Teh. Vjesn. 2018;25(3):701–8.
[39] Yang X-S. Nature-Inspried optimization algorithms. Academic Press; 2020.
[40] Batik Z, Cimen ME, Karayel D, Boz AF. The Chaos-Based Whale Optimization Algorithms Global Optimization. Chaos Theory and Appl 2019;1(1):51–63.
[41] Mirjalili S, Lewis A. The whale optimization algorithm. Adv in engin softw 2016;95:51–67.
[42] Mirjalili S, Mirjalili SM, Lewis A. Grey wolf optimizer. Adv in engin softw 2014;69:46–61.
[43] Mirjalili S. SCA: a sine cosine algorithm for solving optimization problems. Knowl Based Syst 2016;96:120–33.
[44] Çimen ME, et al. Ölü Zamanlı Sistemlerde kullanılan Smith Predictor için Balina Sürüsü Optimizasyonu ile PID Tasarımı. Acad Perspect Proced 2019;2(3):583–92.
[45] Çimen ME. Modelling and Control of Time Delay Systems MsC Thesis. Institue of National; 2018.
[46] Poorani VJ, Vijay Anand LD. Comparison of PID controller and Smith predictor controller for heat exchanger. IEEE International Conference ON Emerging Trends in Computing, Communication and Nanotechnology (ICECCN); 2013.
[47] T. Yücelen, “Uzun ölü zamanli sistemler için smith öngörücüsü yöntemi ile pi-p kontrolör tasarimi”.
[48] Gurban EH, Gheorghe-Daniel A. Comparison of modified Smith Predictor and PID Controller tuned by genetic algorithms for greenhouse climate control. 9th IEEE International Symposium on Applied Computational Intelligence and Informatics (SACI) IEEE; 2014.